**Solid Freeform Fabrication 2022: Proceedings of the 33rd Annual International Solid Freeform Fabrication Symposium – An Additive Manufacturing Conference**
**Reviewed Paper**

# Coalescence behavior of polyamide 12 as function of zero-shear viscosity and influence on mechanical performance

S. Cholewa*[a,b], A. Jaksch*[a,b], D. Drummer

[a] Collaborative Research Center - Additive Manufacturing (CRC 814), Friedrich-Alexander-Universität Erlangen-Nürnberg, Am Weichselgarten 10, 91058 Erlangen, Germany

[b] Institute of Polymer Technology (LKT), Friedrich-Alexander-Universität Erlangen-Nürnberg, Am Weichselgarten 10, 91058 Erlangen, Germany

## Abstract

The favored material for powder bed fusion of polymers (PBF-LB/P) is polyamide-12. Its molecular weight increases from post-condensation at elevated temperatures in the building chamber, consequently having different properties when reused. An important aspect of PBF directly affected hereby is the coalescence behavior, as it significantly determines the surface quality, porosity, and thus the component's mechanical properties. However, detailed studies on coalescence are limited to virgin powders with low viscosity; therefore, coalescence behavior of polyamide-12 with different molecular weights is investigated using hot stage microscopy. Additionally, the zero-shear viscosity is determined using the Carreau model, allowing comparison of experimental results to sintering models. Furthermore, the mechanical properties and surface qualities are analyzed, and components with adequate values are made with two-cycle reprocessed powder. Since surface flaws do not exist uniformly across all components, the orange peel effect is not attributed solely to the increased viscosity of the reused powder.

## Introduction

The term "Additive Manufacturing" refers to a wide range of technologies that all share a unique building method; it is a form of manufacturing where the three-dimensional (3D) product is built into its designed shape using a layer-by-layer approach directly from a computer-aided design (CAD) model [1]. This makes AM fundamentally different from conventional formative or subtractive methods, because it is a tool-free process, and it has several independent units creating a significantly larger degree of complexity in terms of cost-effectiveness. In the beginning, a thin layer of powder, previously heated to the designated process temperature, is spread with a roller or blade onto the platform inside the building chamber all while being under an inert gas causing partial melting and compaction of the particles. The fusing of the melted particles has a critical impact on the porosity of the manufactured part, and thereby on the mechanical performance [2]. Since the process takes place under atmospheric pressure, the coalescence behavior plays a significant role here as the surface tension and viscosity of these particles is the driving factor. Most coalescence models are traced back to Frenkel. For Polyamide 12 in PBF, it is known that one of the predominant effects of process-induced ageing is post-condensation with linear chain growth yielding an increase in viscosity [3]. Although there are many studies on its influence of ageing and mechanics, the coalescence behavior of aged powders has never been directly evaluated. Many studies only consider aged powder for qualitative statements like shifting the melting onset to higher temperatures and extending the coalescence time compared to virgin powder [4]. Furthermore, there are not many precise mechanical parameters for viscosities; rather, there are only generalizations about the process, such as the requirement that low viscosity is needed to achieve good coalescence with no porosity remaining in the fused regions. However, there are little investigations into the viscosities with which components are still produced and what properties they exhibit. The presumed "orange peel" surface flaw is said to be a result of high viscosities, so it is crucial to comprehend powder with increased molecular weight and investigate the surface to establish process quality rules. The purpose of this paper is to describe the coalescence behavior of various aged PA12 powders with differing molecular weights, and their resulting mechanical performance and surface effects.

## State of the Art

Coalescence is a phenomena by which at least two drops of a liquid or melt merge during contact to form a lager single particle [5]. The first studies were carried out by Frenkel [6]. Since the model is only valued at early stages of coalescence as the change of the particle radius is not considered, different authors adopted that model, and all determined that the properties of viscosity and surface tension are the determining factors. The coalescence behavior of two particles is fitted with the modified Frenkel model for viscous sintering of liquids under isothermal conditions given by [7]:

$$\frac{d\theta}{dt} = \frac{\Gamma}{r_o \eta} \frac{2^{-5/3} \cos\theta \sin\theta \, (2 - \cos\theta)^{1/3}}{(1 - \cos\theta)(1 + \cos\theta)^{1/3}}$$

where Γ is the surface tension, η is the viscosity, $a_0$ is the particle radius, θ is the angle between the line connecting the particle centers and that connecting a particle center with the extreme point of the neck.

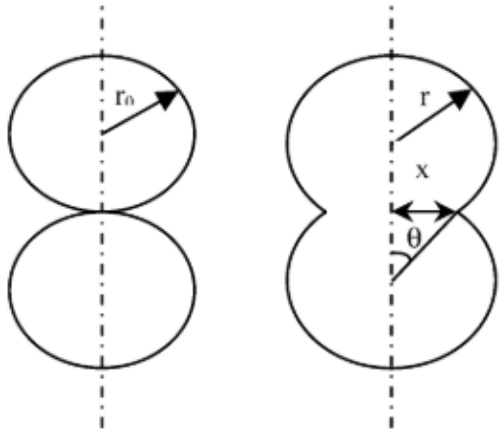


Figure 1: Modified Frenkel model according Pokluda et al. [7]

Many authors have determined the behavior for materials and temperatures for PBF. Zhao et al. [8] showed that for virgin PA12, the Pokluda model describes the coalescence behavior sufficiently, and for measured surface tension, only a small effect of the temperature was observed. Haworth et al. [9] compared the viscosity of virgin PA12 powder with mixed powder (oven test 170 °C 5 h), and observed an increase in viscosity, and furthermore, calculated with the Frenkel model, the sintering kinetics. Another paper dealing with coalescence behavior for PA12 by Chatham et al. [10] focused on different process parameters and their influence on mechanical properties and density. For this purpose, the temperature in the process was observed with the aid of a thermal camera, and the necessary temperature-dependent characteristic values were taken from the literature to calculate the sintering process. Dadbakhsh [2] demonstrated that aged PA12 powder melts at slightly higher temperatures in hot stage microcopy for dynamic measurements with a heating rate of 10 K/min. Berreta et al. [11] investigated the necking time of high temperature materials PEEK and PEK using different MFI and hot stage microscopy processes. The authors determined that the lower molecular weight PEK fuses much faster (roughly by a factor of 2), but the tensile strength is reduced by 30%. According to Haeri [12], the aspect ratio of the parts has an impact on PEK. Plummer [13] investigated the effect of re-used elastomer powder and found that it had no effect on the hot stage microscopy or the mechanical behavior. Benedetti [14] was the first to describe different approaches for using diameter to calculate neck growth. More important, the use of different substrate plates for hot stage microcopy was determined, and only minor deviations were seen. Furthermore, the diameter of the particle decreased as the temperature increased on a heating ramp.

## Experimental

In this work, the common Polyamide 12 (PA2200, EOS GmbH) was investigated in three different stages, and processing tests were carried out without refreshing the powder. This technique resulted in a comparable temperature-time load in the used powder. Starting with virgin powder, three processing cycles were produced. In the first cycle, three construction jobs were fashioned, in the second, two construction jobs, and in the third cycle one construction job. Each building job was 15.5 h; the according building time for each cycle is presented in Table 1.

Table 1: Materials used

| Cycle Number | Count Build Jobs | Starting Powder | Refreshing | Cumulative Building Time |
|---|---|---|---|---|
| 1 | 3 | Virgin powder | No | 15.5 h |
| 2 | 2 | Powder cycle 1 | No | 31 h |
| 3 | 1 | Powder cycle 2 | No | 46.5 h |

### Processing

The processing was carried out on a Formiga P 110. Figure 1 (right) shows the construction job layout used. For the detection of local component properties, test specimens were manufactured in the xy and z directions. The resulting job height is 250 mm, and the filling level is 7.4 % by volume. Per each construction job, a total of 86 multi-purpose test specimens according to DIN EN ISO 527-1 type A were manufactured to determine mechanical properties under tensile load, and 91 80x4x10 mm³ test specimens were used to determine the component density with the following parameter settings

| | |
|---|---|
| Heating time before start of job | 2.5 h |
| Resulting construction time | 15.5 h |
| Cooling time | 10 h |
| Exposure parameters | EOS Standard |
| Building bed temperature | 168 °C |
| Builder chamber temperature | 150 °C |
| Layer Thickness | 0.1 mm |

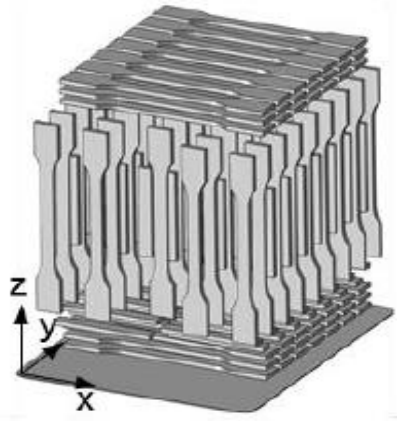


Figure 2: Process parameters (left) and Build job layout (right)

### Viscosity Number

The viscosity number was determined by means of an Ubbelohde viscosimeter according to DIN EN ISO 307. Sulfuric acid was used as the solvent instead of the m-cresol specified in the standard. For each building job, three random samples were analyzed.

### Component Density

The component density was determined using the weighing method on the components (see [15]). The component's width and thickness were determined with a micrometer (± 0.001 mm) at three points, the component length was determined with a digital caliper (± 0.01 mm), and the component weight with a precision balance (± 0.001 g).

### Rheometer

To understand the difference between the starting powders during the process, the zero-shear viscosity was determined by means of frequency sweeps in oscillation mode with a deformation γ of 0.005 via Carreau model at three different temperatures (200, 210 and 220 °C). The measurements were carried out on rational rheometer

(HAAKE Mars 60) equipped with a 25 mm diameter; for quick and good thermal settings, the rheometer is equipped with a heated upper plate. All measurements were conducted in the linear viscoelastic (upper limit $\gamma$ 0.0045) range that was determined by amplitude sweeps. Immediately after post condensation takes place, conventional mold sample preparation is not possible. Instead, powder tablets were prepared with a press to guarantee consistent loadings and improve the consistency of the measurements. Furthermore, the samples were dried for one week in a vacuum oven at 70 °C. The complex viscosity $\eta^*$ was used to characterize the flow behavior as simple polymers are known to obey the Cox-Merz rule [16].

**Hot Stage Microscopy**

Hot microscopic observations for the sintering of polymer particles were performed using a Linkam FTIR600 heating and freezing microscope stages, controlled with central processor Linksys 32 software. A glass plate was used as the substrate for the sintering particles. Two polyamide 12 particles from each cycle of approximately equal size were placed on the stage at ambient temperature and heated up to the isothermal temperatures of 200 °C and 210 °C with the max. heating rate of 150 °C. Preliminary tests ensured that the particles are homogeneously heated by the minimal wetting of the sample carrier with silicon lubricant [17]. The analysis of the experiments was performed using ImageJ software. Here, the sinter growth over time was evaluated by determining the dimensionless parameter of the sinter neck radius. Then the modified Frenkel model was solved in MATLAB by classical Runge-Kutta- method and compared with the experiments.

## Results

### Powder Characteristics

*Viscosity Number*

The measured viscosity numbers (VN) of the new and used powders are shown in Figure 3. It is seen that the viscosity number increases with each processing cycle, starting from VN = 60 ml/g for new powder to 136 ml/g after three processing cycles. With each processing cycle, the rate of change of VN decreases, and the viscosity number approaches a limit value. The increase in the viscosity number is attributed to post-condensation in the solid phase [18]. Due to the temperature-time stress during the process, the chain ends of the Polyamide 12 can react with each other, splitting off water. This leads to an increase in the molecular weight and a concomitant increase in the melt viscosity of the material.

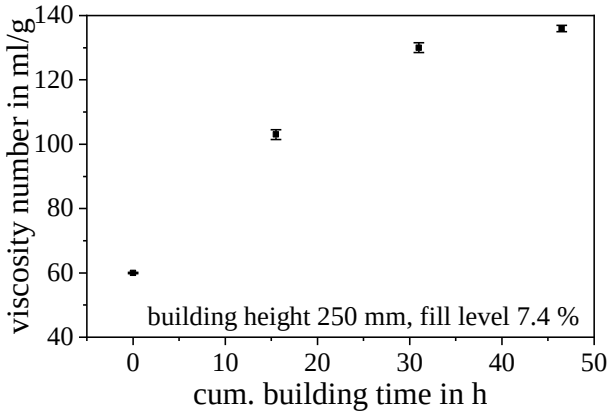


*Figure 3: Viscocity number in dependence of cumulative building time (n=3)*

*Hot Stage Microscopy*

In Figure 4, the isothermal hot stage measurements for the different cycles at a temperature of 200 °C are shown. It is seen that the coalescence behavior is increasing significantly with increasing powder state. The fusing time for cycle 1 (virgin powder) is only a few seconds, whereas for cycle 2, the necking area forms after 10 s. For cycle 3, the necking area has only just formed after a time span of 30 seconds, and for complete fusing, almost 5 minutes was necessary. Dadbakhsha et al. [4] was also able to observe optical differences in the melted particles. It is assumed that the underlying cause may be added additives or optical artefacts.

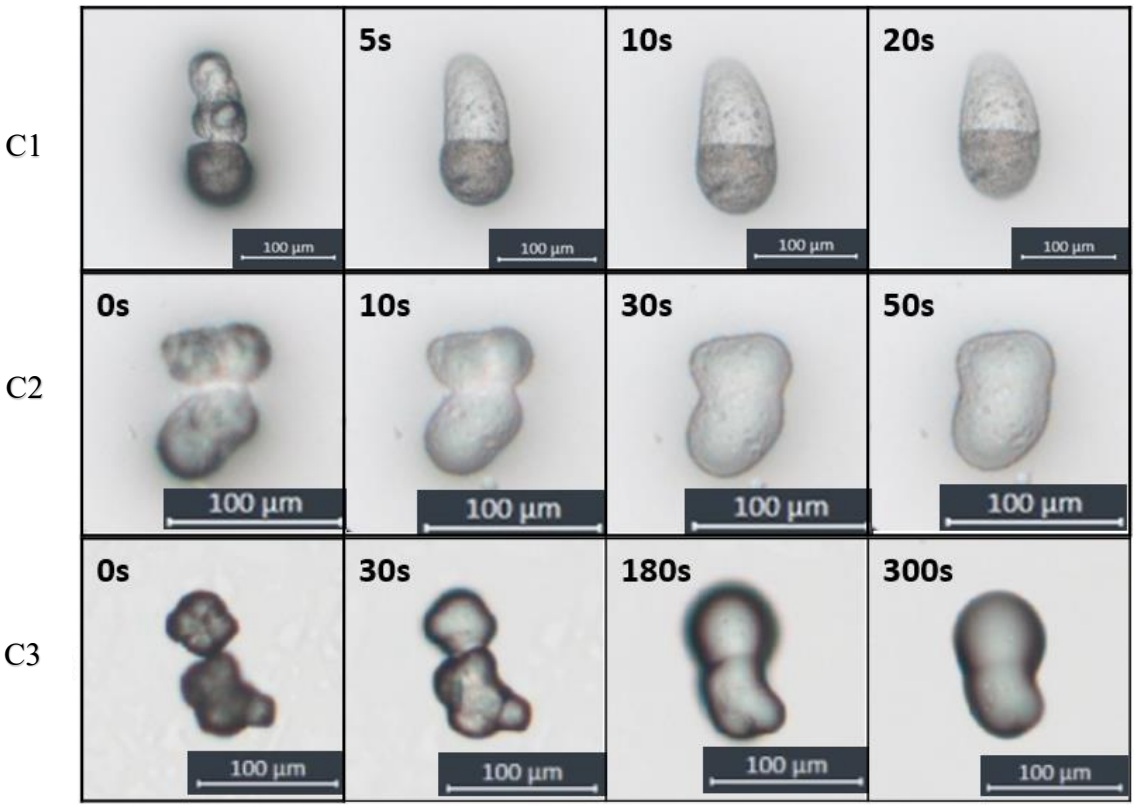


*Figure 4: Coalescence behavior at 200 °C for particles of different cycles*

*Viscosity Measurements*

Figure 5 shows the different viscosity measurements conducted with the rheometer of the different powder states. The loss and storage modulus dependence of the angular frequency of the different powders is depicted at 200 °C on left, the crossover point (COP) of these moduli is an indicator for the molecular structure of the samples as with increasing molecular weight the storage modulus increases and the COP moves to lower frequencies [19]. For cycle 1, no COP occurs at 200 °C, this is a result of the chains being so short that the storage modulus does not intersect that of the loss modulus even for the maximum possible instrument angular frequency of 628 rad/s. Because of the known post-condensation of the powder, the crossover point is detected for cycle 2, which shifts to even lower angular velocities for cycle 3. The zero-shear viscosity of the powders for 210 °C are displayed in the center. The measurements are in strong agreement if the increase of the different states is considered. With increasing cycle length, the increase in the zero-shear viscosity reduces. It must be noted that the zero-shear viscosity cannot be analyzed by oscillation mode at temperatures lower than 210 °C, as the molecular weight of the powder is too high, and thereby the plateau is not reached as shown in Fig. 5 (right) for a temperature of 200 °C.

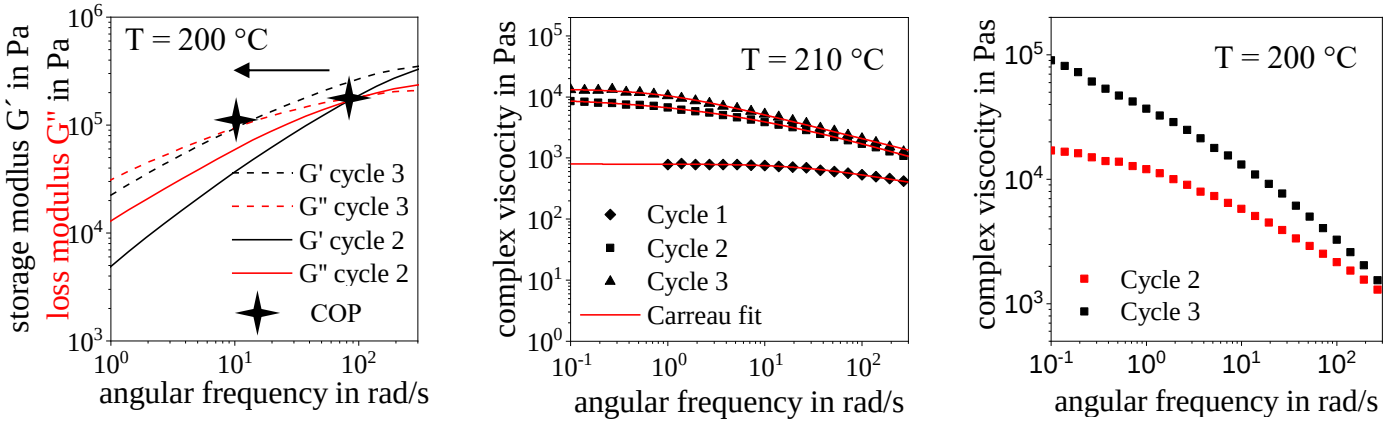


*Figure 5: Rheometer measurements, change cross-over at 200 °C (left), frequency sweeps at 210 °C (center) and 200°C (right)*

*Coalescence Behavior Experiments*

The first isothermal temperature for evaluating the neck-growing radius at 200 °C is shown in Fig. 6 (left). As already illustrated in Fig.5, the progress of the neck radius shows extreme differences among the different powder states. Already seen in Cycle 1, sintering was observed at 196 °C; therefore, the measurement began already at a neck ratio of 0.2 However, the coalescence is completed after 7 seconds, which aligns with previous measurements of the virgin PA12 powder [20]. When considering the other two systems, the coalescence time to achieve a similar dimensionless radius is increased by one magnitude. For Cycle 3, there was a change detectable after 3 minutes, so a plateau was reached only after 240 s. For the second investigated temperature of 210 °C, cycle 1 was completely fused by reaching the holding temperature even with a high heating rate of 150 K/min. Therefore, the coalescence progress at 210 °C is only shown for cycle 2 and cycle 3. In comparison to the first holding temperature, now cycle 2 and 3 are already partly melted and show already a necking during the heating up phase. The progress at the beginning shows a faster process, as expected, but the significant difference to 200 °C occurs towards the end, where the time to reach the plateau is halved. For the models, the previously determined viscosities were used as input variables and the surface tensions (35.6 mN/m) were used for new powders from the literature [21], and kept constant for all cycles. This simplification is permissible after the surface tension only has a weak function of temperature and molecuarl weight [22] in comparison to the the zero-shear viscoity. The resutls for the modfied Frenkel model at 210 °C are shown in Fig. 6 (right).

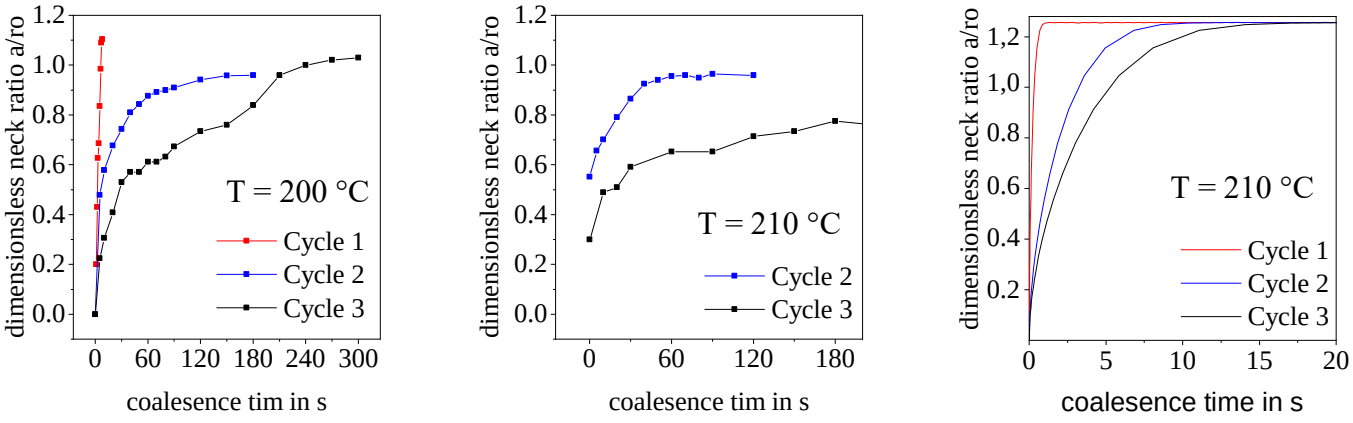


*Figure 6: Dimensionless neck ratio at 200 °C (left) and 210 °C, comparison with Pokluda model*

It is immediately noticeable that ratios around 1 and smaller are achieved in the experiments, whereas the models achieve ratios of 1.26; these deviations are known and discussed in the literature [23]. It is worth noting that for all experiments, irrespective of temperature or viscosity, progress is faster in the model than observed on the hot stage microscopy. Whereas the model predicts the neck ratio in a comparable time for cycle 1, but the differences increase for cycle 2 and 3 significantly.

## Part Characteristics

*Part Density*

Figure 7 shows the measured global component densities of the three processing cycles over the cumulative build time of the initial powder. A distinction is made here between specimens built in the xy and z directions. The component densities in both the xy and z directions are strongly dependent on the ageing state of the starting powder. The component density drops in the xy-direction from approx. 0.95 g/cm³ to 0.83 g/cm³. In the z-direction, this drop is more pronounced, with the component density falling from 0.92 g/cm³ to 0.72 g/cm³. Furthermore, the standard deviation of the component density increases due to a decreasing bulk density and an associated increase in the initial pore diameter, as well as an increase in surface roughness up to the "orange peel".

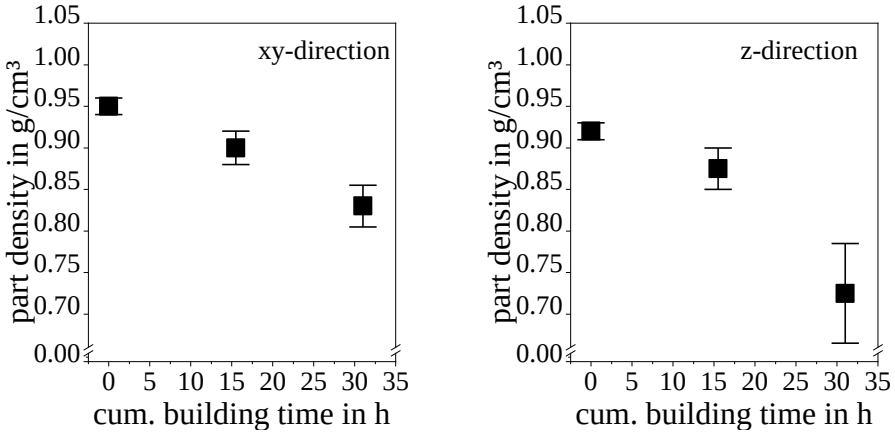


*Figure 7: Component density depending on the ageing status of the starting powder*

*Part Surface*

An analysis of the parts in z- direction illustrates that the surface flaw "orange peel" occurs for cycle 2 at front and back position. In the next cycle, positions of the parts with orange peel increases; however, even with a starting powder which has experienced 31 h of building time, parts without any surface flaws are produced.

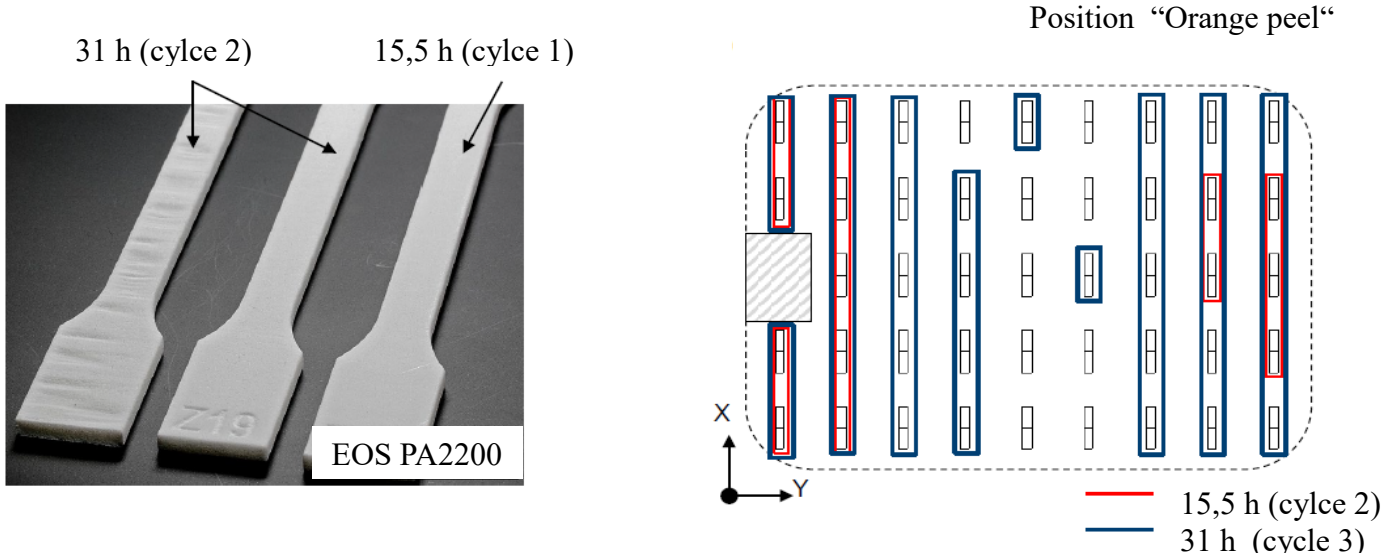


*Figure 8: Orange peel in dependence of part position and starting powder*

*Mechanical Performance*

There is a significant decrease of the elongation at break and the yield stress for z tension samples. Smaller decrease with in xy direction. In general z tension samples react more sensitively to aged powder. A substantial decrease of the elongation at break and the yield stress for z tension samples are observed, and the distribution of the elongation at break largely increases with cumulative construction time. For cycle 3, the mechanics were not investigated after the density results dropped and increased surface defects occurred.

Table 2: Mechanical Characteristics

| Cycle nr. | Build direction | UTS in MPa | Elongation at break in % |
|---|---|---|---|
| Cycle 1 | xy | 51.22 (± 1.3) | 15.78 (± 3.38) |
| | z | 48.35 (± 0.77) | 11.28 (± 3.38) |
| Cycle 2 | xy | 47.96 (± 1.05) | 15.16 (± 2.53) |
| | z | 22.26 (± 12.82) | 4.24 (± 6.6) |

## Summary and Outlook

This study presents a theoretical and experimental investigation of the sintering process of commercial polyamide 12 powders as a function of the viscosity. When observing the viscosity number as well as the zero-shear viscosity according to Carreau, it is apparent that the ageing progress is maximum at the beginning and decreases with time seemingly reaching a plateau. The results of the hot stage microscopy show that the growth of the sinter neck agrees with the modelling for the first cycle which is comparable to existing studies The coalescence behavior differs significantly, as cycle 1 powder investigations are not possible at 210 °C, since the particles are already coalesced despite a heating rate of 150 K/min. However, when the results are compared for powders with increasing molecular weights, viscosity deviations detected. The results achieved show a lower rate of coalescence than what the models discussed in this paper predicted. The following points are of importance when considering the manufactured components: the influence of cumulative construction time is more significant for components built in z direction. Additionally, the span of the resulting component density increases with increasing cycle time and is more distinct for z components. The mechanics achieve typical characteristic values for cycle 1. For cycle 2, the UTS demonstrates a strong correlation to the building direction; where in the xy direction changes are small, and the z components only reach values of 50 % in comparison to cycle 1. The surface flaw "orange peel" shows a dependence on the position in the build platform; so, it is the first time for cycle 2 to occur in the rear and front area. However, despite further thermal stress around 15.5 h, and a significant increase in melt viscosity, components are possibly produced in the center without surface defects for cycle 3. This may be attributed to the different position dependent temperature profiles. The experimental coalescence studies confirm that the temperature has a significant influence on coalescence behavior. Here, scientific studies confirm that with adapted process parameters, processing is also possible with aged powder material. Regarding viscosity, it is important to note that a zero-shear viscosity of approx. $8*10^3$ Pas for polyamide 12 at 25 K above melting point $T_m$ ([4]) represents a limit for standard exposure. For further investigations, the coalescence behavior of mixed powders as it is typical in the process must be examined. Furthermore, the findings will be transferred to other material systems for the PBF-LB/P. To enable a general statement to be made about the material requirements in terms of viscosity.


## Acknowledgement

Funded by the Deutsche Forschungsgemeinschaft (DFG, German Research Foundation) – Project-ID 61375930 – SFB 814, sub-project A3, T3.


## References


1. Schmid, M., Laser Sintering with Plastics. Vol. 1. 2018, München: Carl Hanser Verlag.
2. Wegner, A., Theorie über die Fortführung von Aufschmelzvorgängen als Grundvoraussetzung für eine robuste Prozessführung beim Laser-Sintern von Thermoplasten. 2015, Universität Duisburg-Essen.
3. Wudy, K. and Drummer, D., Additive Manufacturing, 2019. 25: p. 1.
4. Dadbakhsh, S., Verbelen, L., Verkinderen, O., Strobbe, D., Van Puyvelde, P., and Kruth, J.-P., European Polymer Journal, 2017. 92: p. 250.
5. Muller, J.D.B., M.; Maazouz, A., Macromolecules, 2008. 41(6): p. 2096.
6. Frenkel, J., Journal of Phyiscs, 1945. vol. 9, : p. 385.
7. Pokluda, O., Bellehumeur, C.T., and Machopoulos, J., AIChE Journal, 1997. 43(12): p. 3253.
8. Zhao, M., Drummer, D., Wudy, K., and Drexler, M., International Journal of Recent Contributions from Engineering, Science & IT (iJES), 2015. 3(1).
9. Haworth, B., Hopkinson, N., Hitt, D., and Zhong, X., Rapid Prototyping Journal, 2013. 19(1): p. 28.
10. Chatham, C.A., Bortner, M.J., Johnson, B.N., Long, T.E., and Williams, C.B., Materials & Design, 2021. 201.
11. Berretta, S., Wang, Y., Davies, R., and Ghita, O.R., Journal of Materials Science, 2016. 51(10): p. 4778.
12. Haeri, S., Benedetti, L., and Ghita, O., Powder Technology, 2020. 363: p. 245.

13. Plummer, K., Vasquez, M., Majewski, C., and Hopkinson, N., Proceedings of the Institution of Mechanical Engineers, Part B: Journal of Engineering Manufacture, 2012. 226(7): p. 1127.
14. Benedetti, L., Brulé, B., Decraemer, N., Evans, K.E., and Ghita, O., Powder Technology, 2019. 342: p. 917.
15. Drummer, D., Drexler, M., and Wudy, K., Procedia Engineering, 2015. 102: p. 1908.
16. Osswald, T.A.R., N.- Polymer rheology fundamentals and applications. 2015.
17. Scribben, E., Baird, D., and Wapperom, P., Rheologica Acta, 2005. 45(6): p. 825.
18. Flory, P.J., PRINCIPLES OF POLYMER CHEMISTRY. 1953, New York: Cornell University Press.
19. Schröder, T., Rheologie der Kunststoffe: Theorie und Praxis. 2018, München: Carl Hanser Verlag
20. Zhao, M.D., D; Wudy, K; Drexler, M. Untersuchung des Schmelz- und Sinterprozesses von Polyamid 12 beim selektiven Strahlschmelzen Investigating the melting and sintering process of polyamide 12 for selective laser melting. in Fachforum „Wissenschaft“. 2015.
21. Wudy, K., Alterungsverhalten von Polyamid12 beim selektiven Lasersintern. 2017, FAU Erlangen-Nürnberg.
22. Moreira, J.C. and Demarquette, N.R., Journal of Applied Polymer Science, 2001. 82(8): p. 1907.
23. Hejmady, P., van Breemen, L.C.A., Anderson, P.D., and Cardinaels, R., Soft Matter, 2019. 15(6): p. 1373.